

# Study Concerning the Energy-to-Mass Ratio in Pneumatic Muscles

Tudor Deaconescu, Andrea Deaconescu

**Abstract**—The utilization of pneumatic muscles in the actuation of industrial systems is still in its early stages, hence studies on the constructive solutions which include an assessment of their functional performance with a focus on one of the most important characteristics—energy efficiency are required. A quality indicator that adequately reflects the energy efficiency of an actuator is the energy-to-mass ratio. This ratio is computed in the paper for various types and sizes of pneumatic muscles manufactured by Festo, and is subsequently compared to the similar ratios determined for two categories of pneumatic cylinders.

**Keywords**—Pneumatic cylinders, pneumatic muscles, energy-to-mass ratio, muscle stroke.

## I. INTRODUCTION

**A**FTER electric current compressed air is the second most important energy generator in industrial actuations. Applications of compressed air go back to the 19<sup>th</sup> century, when the first pneumatic jack hammers were built to be used in mining. The increasingly large scale of the compressed air industrial applications is due to its specific benefits, including [1]:

- compressed air can be generated in any place and quantity;
- high energy density, reduced weight and easy transportation;
- pneumatic energy is easily stored;
- compressed air is non-flammable and carries no risk of explosion;
- pneumatic systems maintenance requires minimum effort, etc.

The disadvantages of compressed air utilisation concern:

- achieving high actuation forces requires large size working equipment;
- the water contained by the compressed air corrodes the components of the installations;
- shocks occur at the end of the piston stroke causing the destruction of the pneumatic motor;
- high energy consumption.

The most frequently deployed effector elements of pneumatic systems are linear or rotation motors with a piston, a membrane or blades. It is the role of these motors to transform the pneumatic energy supplied by the compressed

air into a linear displacement or a rotation.

The construction of linear pneumatic motors with membranes typically includes two casings clamping an oil-resistant rubber membrane. Compared to piston motors, the membrane ones have a number of significant benefits:

- lighter;
- no high manufacturing accuracies required;
- easy sealing, by the very membrane;
- high sensitivity;
- longer service life.

Despite all these advantages, a large-scale utilization of membrane pneumatic motors is limited by the fact that the actuation force is not constant during the length of the stroke.

The utilization of membranes in the construction of pneumatic actuation elements has known a continued development, particularly in relation to the industrial robots. Results worth to mentioning were obtained by the researchers from the Orthopedic Centre of Heidelberg, Germany in 1948, the pneumatic arm developed by the American J.L. McKibben, the stepping robot WAP 1 built by Waseda University Tokyo, Japan in 1969 [2]. The series of these achievements has been recently expanded by the pneumatic muscle, which comes in form of a tube that contracts when fed pressure. The history of this type of pneumatic muscle starts in 1872, when professor Franz Reuleaux described the first flexible pneumatic actuator [2]. It was A. H. Morin who in 1953 patented a first variant of actuator in that a lattice of textile fibers is built into a cylindrical rubber tube [3]. Since then numerous constructive solutions of artificial pneumatic muscles were developed, like the ones put forward by Yarlott and Mass (1972), Takagi and Sakaguchi (1986), Kukolj (1988), Paynter (1988) or Daerden (1999) [4]-[8]. Another constructive variant of a pneumatic muscle is the one developed by Festo of Germany [9].

This paper undertakes a study of Festo pneumatic muscles, with a focus on a characteristic known as the *energy-to-mass* ratio. Conducting such a study is necessary because in literature on pneumatic muscles the high value of this quantity is presented as an advantage, without however offering concrete data or a comparison with the values of this ratio in the case of other types of pneumatic actuators [10]-[12].

Following the introduction, Section II of the paper presents concisely some of the characteristics of pneumatic muscles, followed, in Section III by a description of the methodology used to determine the values of the energy-to-mass ratios for the three types of Festo pneumatic muscles. Section IV includes a comparison of the values of the ratios computed previously with those of cylinders of the same dimensions.

Tudor Deaconescu (Prof. Dr. Eng.) and Andrea Deaconescu (Prof. Dr. Eng.) are with the Transilvania University of Brasov, Faculty of Technological Engineering and Industrial Management, Department of Industrial Engineering and Management, Bd. Eroilor 29, Romania, RO-500036 (phone: 0040-268-477113; fax: 0040-268-477113; e-mail: tdeacon@unitbv.ro, deacon@unitbv.ro).

Conclusions are presented in Section V.

## II. CHARACTERISTICS OF THE PNEUMATIC MUSCLES

Artificial muscles broadly mimic the functioning of the human muscle fiber (Fig. 1), and benefit from a number of characteristics like shock absorbing capacity and shock resistance, low weight, reduced overall size and reduced mass per power unity, elasticity (spring-like behavior) due on one hand to air compressibility and to the variation of force with displacement, on the other, easy connectivity and safe operation.

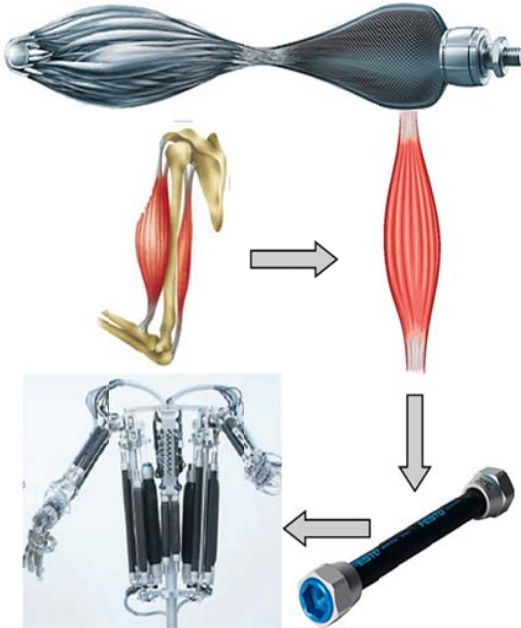


Fig. 1 Pneumatic artificial muscles mimic a biological muscle

Compared to classical piston pneumatic motors, pneumatic muscles have certain advantages like:

- at an identical diameter, considerably higher force;
- superior media resistance;
- for many applications, reduced compressed air consumption;
- any actuator length easy to produce;
- no stick-slip characteristics;
- silent positioning etc.

The main European manufacturer of pneumatic muscles is Festo AG & Co of Germany. The main constructive element of artificial muscles is a chloroprene flexible tube covered by a sealed envelope made from inelastic aramid fibers displayed in diamond patterns, thus forming a 3D-lattice. (Fig. 2) [9].

The interior diameters of the chloroprene tubes are of 10, 20 or 40 mm, resulting in three muscle types, the tube wall thickness varying between one and two millimeters. In small size muscles, the number of fibers is 60 displayed in two layers, while larger muscles have up to 240 fibers. The diameter of each fiber is from 0.1 to 0.3 mm [13], [14]. The precise position of each fiber is remarkable in the construction

of these muscles, so that despite their large number, no fiber touches another.



Fig. 2 Construction and structure of a Festo pneumatic muscle

The mass of the artificial muscles is directly dependent on their length, but, due to the materials used for their construction this mass is significantly smaller than that of a pneumatic cylinder of similar size. Fig. 3 presents the dependencies of the masses of the three types of muscles manufactured by Festo on their lengths. The graph was plotted based on the information extracted from MuscleSIM 2.0.1.5 application, provided by the manufacturer.

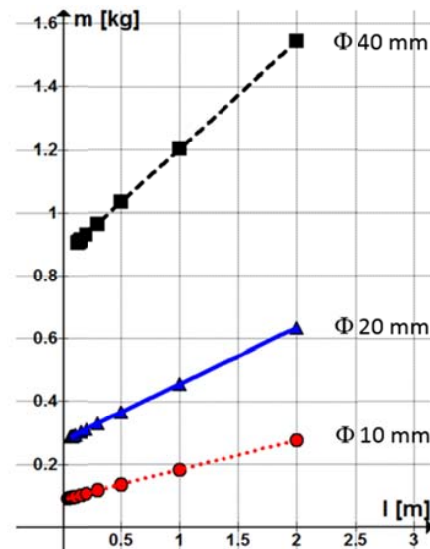


Fig. 3 Dependency of Festo pneumatic muscle mass on muscle length

The linear functions that best describe the dependency of a pneumatic muscle mass on its length are:

$$m_{10}(l) = 0.0939 \cdot l + 0.0882 \quad (1)$$

$$m_{20}(l) = 0.178 \cdot l + 0.277 \quad (2)$$

$$m_{40}(l) = 0.34 \cdot l + 0.8631 \quad (3)$$

The indices attached to the masses denote the interior diameter of the chloroprene tube of each type of muscle.

The mass of pneumatic muscles is a particularly important characteristic where computing the *energy-to-mass ratio* is concerned. Section III of the paper presents the methodology for computing the values of these ratios for the three types of Festo muscles and shows the variation of this characteristic

versus actuator length.

$$R_{\frac{E}{m}} = \frac{l \cdot \int F(\epsilon) \cdot d\epsilon}{m} \tag{5}$$

III. THE ENERGY-TO-MASS RATIO

The energy-to-mass ratio is a quality indicator used for comparing various types of actuators from the viewpoint of their energy efficiency. In 2005 D. Plettenburg provided an expression for this indicator [15]:

$$R_{\frac{E}{m}} = \frac{\int F(s) \cdot ds}{m} \tag{4}$$

where  $F(s)$  is the force developed by the pneumatic muscle depending on its axial contraction  $s$ , and  $m$  is its mass.

This paper puts forward a relationship for computing the energy-to-mass ratio that considers the specific axial contraction  $\epsilon = s/l$  of the pneumatic muscle, as well as its length  $l$ . When inflated by compressed air the pneumatic muscle shortens its length; this shortening is the stroke of the pneumatic muscle, denoted by  $s$ . With these notations, the equation becomes:

Prerequisite to computing the energy-to-mass ratio is determining the equation that describes the variation of the force developed by a pneumatic muscle in dependence on its specific axial contraction. In this regard, based on the information provided by Muscle SIM application it could be noted that for any given pressure (e.g. 0.6 MPa), the force developed by the pneumatic muscle, regardless of its length, varies within the same limits. Table I features these limits for the three types of muscles.

TABLE I  
VARIATION LIMITS OF THE FORCES DEVELOPED BY A PNEUMATIC MUSCLE

| Muscle diameter [mm]        | Φ 10  | Φ 20  | Φ 40  |
|-----------------------------|-------|-------|-------|
| $\epsilon_{min}$            | 0.016 | 0.038 | 0.078 |
| Maximum force $F_{max}$ [N] | 400   | 1200  | 4000  |
| $\epsilon_{max}$            | 0.2   | 0.2   | 0.2   |
| Minimum force $F_{min}$ [N] | 30    | 330   | 1715  |

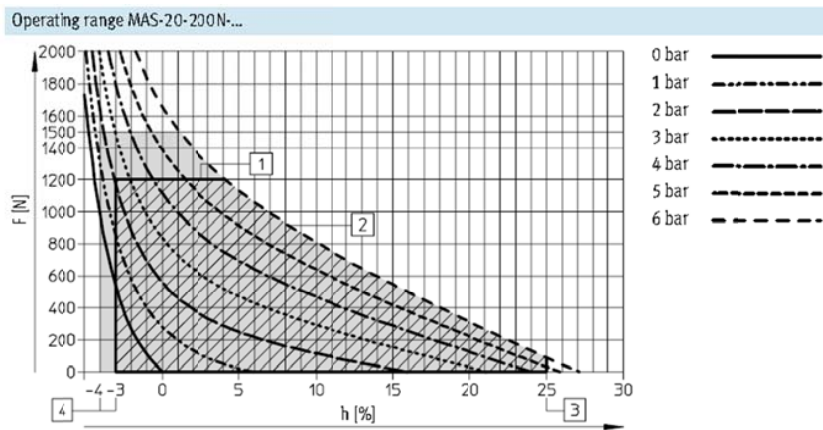


Fig. 4 Nomogram  $F = f(\epsilon)$  corresponding to a 20 mm diameter pneumatic muscle

For each type, dimension of pneumatic muscle  $\epsilon_{min}$  and  $\epsilon_{max}$  denote the specific minimum and maximum admissible axial contractions of these actuators, respectively.

Similar results to those provided by Muscle SIM application are obtained also by analyzing the nomograms corresponding to each type of pneumatic muscle. Fig. 4 exemplifies such a nomogram for a 20 mm diameter pneumatic muscle [16].

Starting from the information in Table I, the curves presented in Fig. 5 were plotted, showing the dependency of the forces developed by the three types of pneumatic muscles versus their specific axial contractions, dependencies described by (6)-(8).

The polynomial functions above have determination coefficients equal to 1 ( $R^2 = 1$ ), what confirms that these relationships describe the studied phenomenon with maximum accuracy.

$$F_{10}(\epsilon) = 3.369 \cdot 10^5 \cdot \epsilon^4 - 1.831 \cdot 10^5 \cdot \epsilon^3 + 3.774 \cdot 10^4 \cdot \epsilon^2 - 5135.05 \cdot \epsilon + 474.4 \tag{6}$$

$$F_{20}(\epsilon) = 1.678 \cdot 10^5 \cdot \epsilon^4 - 1.087 \cdot 10^5 \cdot \epsilon^3 + 2.924 \cdot 10^4 \cdot \epsilon^2 - 8640.755 \cdot \epsilon + 1490.71 \tag{7}$$

$$F_{40}(\epsilon) = 3.681 \cdot 10^5 \cdot \epsilon^4 - 2.829 \cdot 10^5 \cdot \epsilon^3 + 9.985 \cdot 10^4 \cdot \epsilon^2 - 3.37 \cdot 10^4 \cdot \epsilon + 6136.78 \tag{8}$$

Knowing the relationships for the forces further on the expressions for the energy developed by the pneumatic muscles are determined. Figs. 6-8 show the working range for each type and dimension of pneumatic muscle underlying the determined mathematical relationships for the energies.

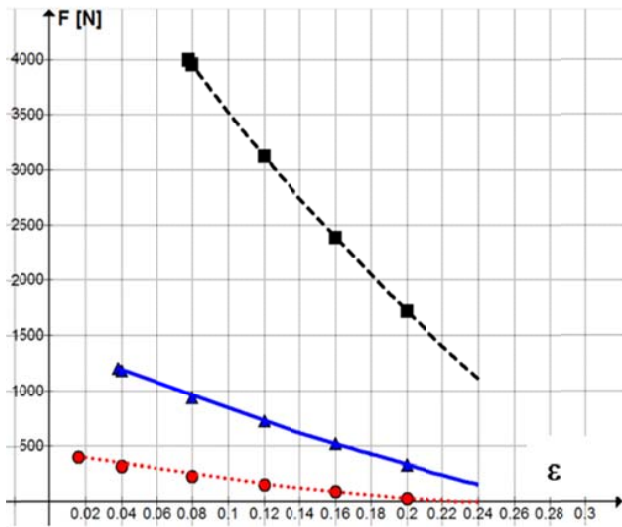


Fig. 5 Dependency of the force developed by a pneumatic muscle on its specific axial contraction  $\varepsilon$

The equations of the energy developed by the pneumatic muscles are:

$$E_{10}(l) = l \cdot \int_{0.016}^{0.2} F_{10}(\varepsilon) \cdot d\varepsilon = 34.1421 \cdot l \quad (9)$$

$$E_{20}(l) = l \cdot \int_{0.038}^{0.2} F_{20}(\varepsilon) \cdot d\varepsilon = 119.6437 \cdot l \quad (10)$$

$$E_{40}(l) = l \cdot \int_{0.078}^{0.2} F_{40}(\varepsilon) \cdot d\varepsilon = 340.3839 \cdot l \quad (11)$$

Upon introducing (1)-(3) and (9)-(11) into (5) the energy-to-mass ratios for the three dimensions of pneumatic muscles can be computed.

$$R_{\frac{E}{m},10} = \frac{E_{10}(l)}{m_{10}(l)} = \frac{34.1421 \cdot l}{0.0939 \cdot l + 0.0882} \quad (12)$$

$$R_{\frac{E}{m},20} = \frac{E_{20}(l)}{m_{20}(l)} = \frac{119.6437 \cdot l}{0.178 \cdot l + 0.277} \quad (13)$$

$$R_{\frac{E}{m},40} = \frac{E_{40}(l)}{m_{40}(l)} = \frac{340.3839 \cdot l}{0.34 \cdot l + 0.8631} \quad (14)$$

Fig. 9 features the curves that describe the dependency of the energy-to-mass ratio on the length of the pneumatic muscle for each muscle diameter.

Equations (12)–(14) as well as the curves of Fig. 9 reveal that the energy-to-mass ratios of pneumatic muscles increase with muscle length, *i.e.* with the magnitude of the capable stroke.

The above results gain relevance when compared to other pneumatic actuators. Such comparison is conducted in Section IV of the paper, the selected actuators being two single-acting cylinders.

#### IV. THE ENERGY-TO-MASS RATIO IN SINGLE-ACTING CYLINDERS

The two pneumatic cylinders selected for determining the energy-to-mass ratio belong to the ESNU and to the compact range ISO 21287 (model AEN), respectively, are single-acting, with a selected piston diameter of 20 mm, and a maximum stroke of 25 mm.

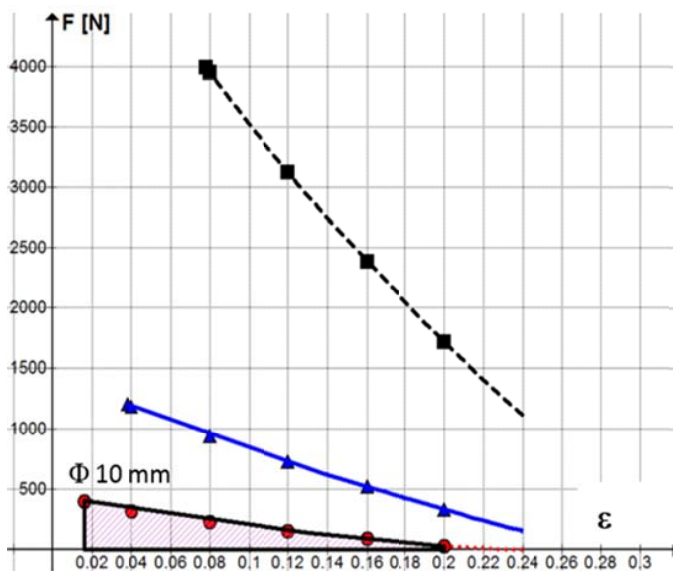


Fig. 6 Working range of the Festo MAS-10-N Fluid Muscle

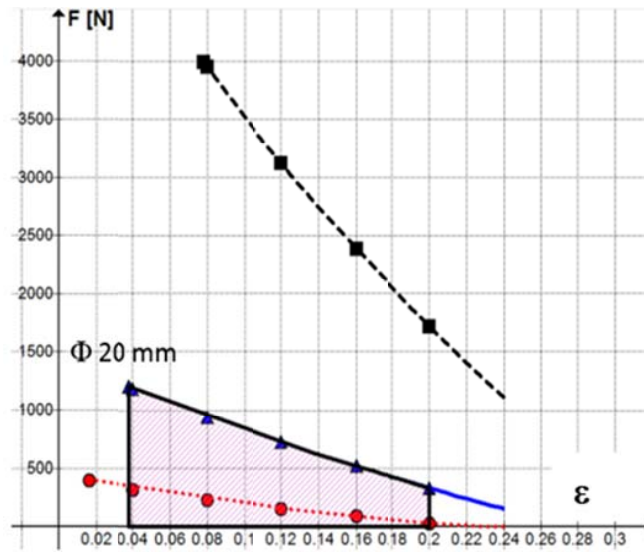


Fig. 7 Working range of the Festo MAS-20-N Fluid Muscle

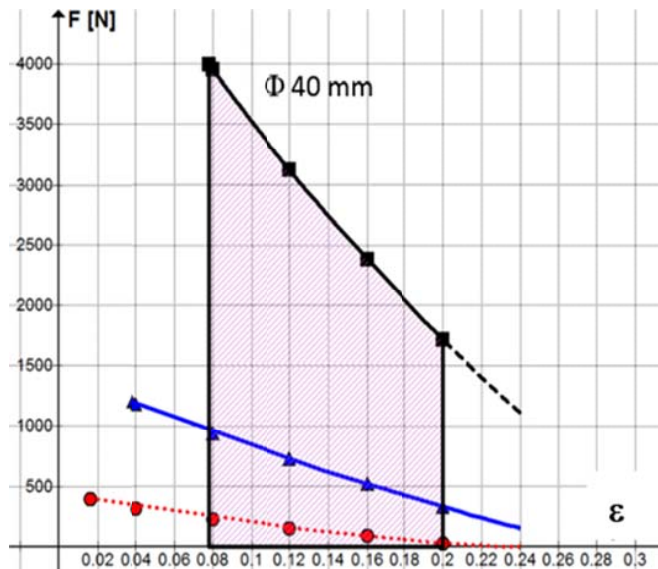


Fig. 8 Working range of the Festo MAS-40-N Fluid Muscle

For the pneumatic cylinders, Table II features the characteristics of interest for the computation of the energy-to-mass ratio.

TABLE II  
CHARACTERISTICS OF THE ESNU AND AEN PNEUMATIC CYLINDERS

| Cylinder type                               | ESNU   | AEN   |
|---|--------|-------|
| Developed force at 0.6 MPa [N]              | 169    | 152   |
| Mass corresponding to a 0 mm stroke [kg]    | 0.167  | 0.131 |
| Additional mass for every 10 mm stroke [kg] | 0.0072 | 0.021 |

Starting from these data, the linear functions that describe the dependency of the mass of such a pneumatic cylinder on the conducted stroke ( $s$ ) can be determined.

$$m_{ESNU}(s) = 0.0072 \cdot s + 0.167 \quad (15)$$

$$m_{AEN}(s) = 0.021 \cdot s + 0.131 \quad (16)$$

The computational relationships of the energy-to-mass ratios of these cylinders are:

$$R_{\frac{E}{m}ESNU} = \frac{F \cdot s}{m} = \frac{169 \cdot s}{0.0072 \cdot s + 0.167} \quad (17)$$

$$R_{\frac{E}{m}AEN} = \frac{F \cdot s}{m} = \frac{152 \cdot s}{0.021 \cdot s + 0.131} \quad (18)$$

Starting from (17) and (18), Fig. 11 shows the dependencies of the energy-to-mass ratios on the strokes of the two pneumatic cylinders.

In order to observe the differences between the energy efficiencies of a pneumatic muscle and a pneumatic cylinder,

respectively, Table III features a comparison of the computed values of the energy-to-mass ratios of a 20 mm diameter pneumatic muscle and of the previously analyzed cylinders.

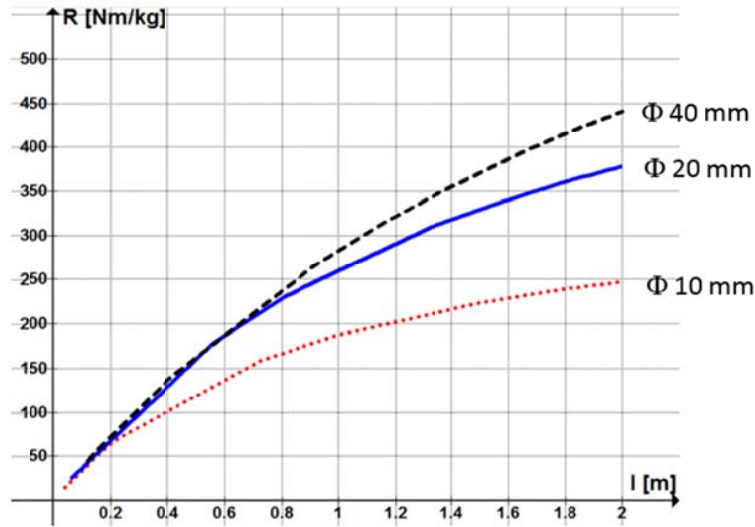


Fig. 9 Dependency of the energy-to-mass ratios on the lengths of the pneumatic muscles



Fig. 10 ESNU and AEN (Festo) type pneumatic cylinders

TABLE III  
COMPARISON BETWEEN THE VALUES OF THE ENERGY-TO-MASS RATIOS

| Stroke [mm] | Actuator type              |       |       |
|-------------|----------------------------|-------|-------|
|             | Pneumatic muscle $\Phi 20$ | ESNU  | AEN   |
|             | $R_{Em}$                   |       |       |
| 0           | -                          | 0     | 0     |
| 5           | -                          | 5.05  | 5.79  |
| 10          | -                          | 10.11 | 11.58 |
| 15          | 30.90                      | 15.17 | 17.36 |
| 20          | 40.58                      | 20.22 | 23.13 |
| 25          | 49.97                      | 25.27 | 28.89 |

The data in Table III allow the plotting of the variation diagrams of the energy-to-mass ratio versus the stroke of the three actuators. Fig. 12 presents these dependencies.

The analysis, Fig. 12, confirms the assertions found in literature, in the studies on pneumatic muscles, namely that this type of pneumatic actuator ensures a higher energy-to-mass ratio than other types of pneumatic motors of similar dimensions. Consequently, from the viewpoint of energy efficiency the utilization of pneumatic muscles is recommended in applications requiring the generation of a certain force while keeping the weight of the assembly at a minimum.

V. CONCLUSION

The study presented and discussed in the paper, concerning the devising of a methodology for computing the energy-to-mass ratio for different pneumatic actuators demonstrates that, although yet insufficiently known and deployed, pneumatic muscles offer numerous benefits. In-depth knowledge of their performance will enable the replacement of single-acting cylinders by pneumatic muscles in an increasing number of applications.

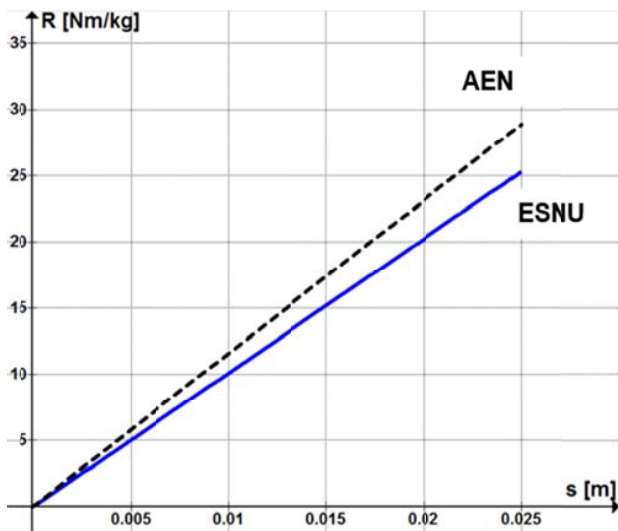


Fig. 11 Dependency of the energy-to-mass ratios on the stroke of the pneumatic cylinders

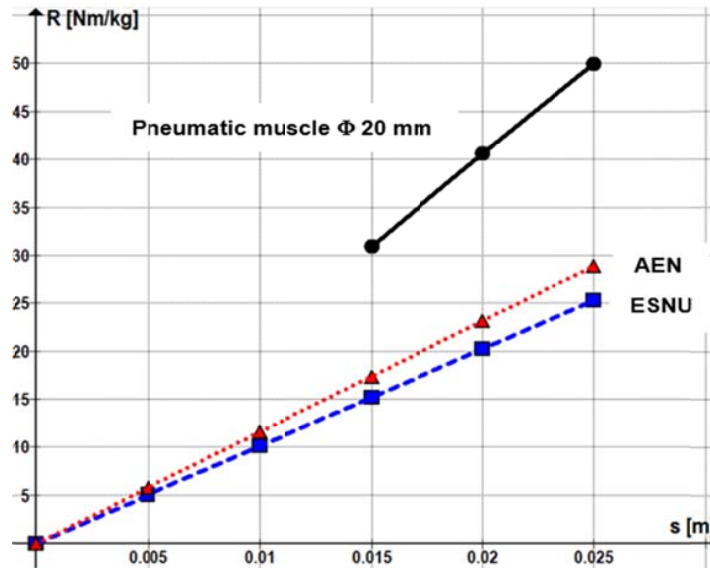


Fig. 12 Comparison between the evolutions of the energy-to-mass ratios versus the stroke of the three types of actuators

#### REFERENCES

- [1] E. Pashkov, Y. Osinskiy, A. Chetviorkin, *Electropneumatics in Manufacturing Processes*. Isdatelstvo SevNTU Sevastopol, 2004.
- [2] S. Hesse, *The Fluidic Muscle in Application*. Blue Digest on Automation, Esslingen, 2003
- [3] A.H. Morin, Elastic Diaphragm. U.S. Patent No. 2642091, 1953.
- [4] J.M. Yarlott, H. Mass, Fluid Actuator. U.S. Patent No. 3645173, 1972.
- [5] T. Takagi, Y. Sakaguchi, Pneumatic Actuator for Manipulator. U.S. Patent No. 4615260, 1986.
- [6] M. Kukulj, Axially Contractible Actuator. U.S. Patent No. 4733603, 1988.
- [7] H.M. Paynter, Hyperboloid of Revolution Fluid-Driven Tension Actuators and Method of Making. U.S. Patent No. 4721030, 1988.
- [8] Daerden, F., *Conception and Realization of Pleated Pneumatic Artificial Muscles and Their Use as Compliant Actuation Elements*. Ph.D. Thesis, Vrije Universiteit Brussels, Brussels, Belgium, 1999.
- [9] Fluidic Muscle DMSP/MAS, Festo Product Flyer, 2015, [https://www.festo.com/net/SupportPortal/Files/340809/Muskel\\_Flyer\\_en.pdf](https://www.festo.com/net/SupportPortal/Files/340809/Muskel_Flyer_en.pdf)
- [10] N. Tsagarakis, D.G. Caldwell D.G., "Improved modelling and assessment of pneumatic muscle actuators," in *Proc. of the IEEE International Conference on Robotics & Automation*, April 2000, San Francisco, USA, pp. 3641-3646.
- [11] N. Nakamura, M. Sekiguchi, K. Kawashima, T. Fujita, T. Kagawa, "Developing a robot arm using pneumatic artificial rubber muscles," in *Bath Workshop on Power Transmission & Motion Control*, 2002.
- [12] G.A. Medrano-Cerda, C.J. Bowler, D.G. Caldwell, "Adaptive position control of antagonistic pneumatic muscle actuators," in *Proc. of the IEEE/RSJ International Conference on Intelligent Robots and Systems*, Pittsburgh, USA, 1995, pp. 378-383.
- [13] Festo: Precisely to the point: membrane technology, (2014) [https://www.festo.com/cms/en\\_corp/14047.htm](https://www.festo.com/cms/en_corp/14047.htm)
- [14] M. Santora, Membrane technology flexes its muscle – precisely, Pneumatic Tips. A Fluid Power World Resource, 2015.
- [15] D.H. Plettenburg, "Pneumatic Actuators: a Comparison of Energy-to-Mass Ratio's", in *Proc. of the 2005 IEEE 9th International Conference on Rehabilitation Robotics*, Chicago, IL, USA, 2005, pp. 545-549.
- [16] Festo Fluidic Muscle DMSP/MAS, [https://www.festo.com/rep/en\\_corp/assets/pdf/info\\_501\\_en.pdf](https://www.festo.com/rep/en_corp/assets/pdf/info_501_en.pdf)